Isotopic compositions in projectile fragmentation at Fermi energies*

Nihal Buyukcizmeci[1], A. Ergun[1], H. Imal[1], R. Ogul[1], A.S. Botvina[2,3]

[1]*Selcuk University, Department of Physics, 42079, Campus, Konya, Turkey*
[2]*Frankfurt Institute for Advanced Studies, J.W. Goethe University, D-60438 Frankfurt am Main, Germany*
[3]*Institute for Nuclear Research, Russian Academy of Sciences, 117312 Moscow, Russia*

September 22, 2015
International School of Nuclear Physics/Workshop on
"Probing Hadron Structure with Lepton and Hadron Beams", 16-24 September 2015, Erice, ITALY

*This work is supported by Tübitak-113F058 project and Selcuk U. BAP- 15701520

Content

1. Introduction
2. Statistical Multifragmentation Model
3. Angular momentum and Coulomb effects for hot fragments in peripheral HICs at Fermi energies
4. Interpretation of FAZIA[1] experimental data with new approach
5. Conclusions

[1]. S. Barlini, S. Piantelli, et al., Phys. Rev. C **87**, (2013) 054607

Statistical approach in nuclear reactions:conception of equilibrium

Experimentally established: 1) few stages of reactions leading to multifragmentation, 2) short time ~100fm/c for primary fragment production, 3) freeze-out density is around $0.1\rho_0$ -$0.6\rho_0$, 4) high degree of equilibration at the freeze-out.

Intermediate energy collisions

Preequlibrium emission + equilibration

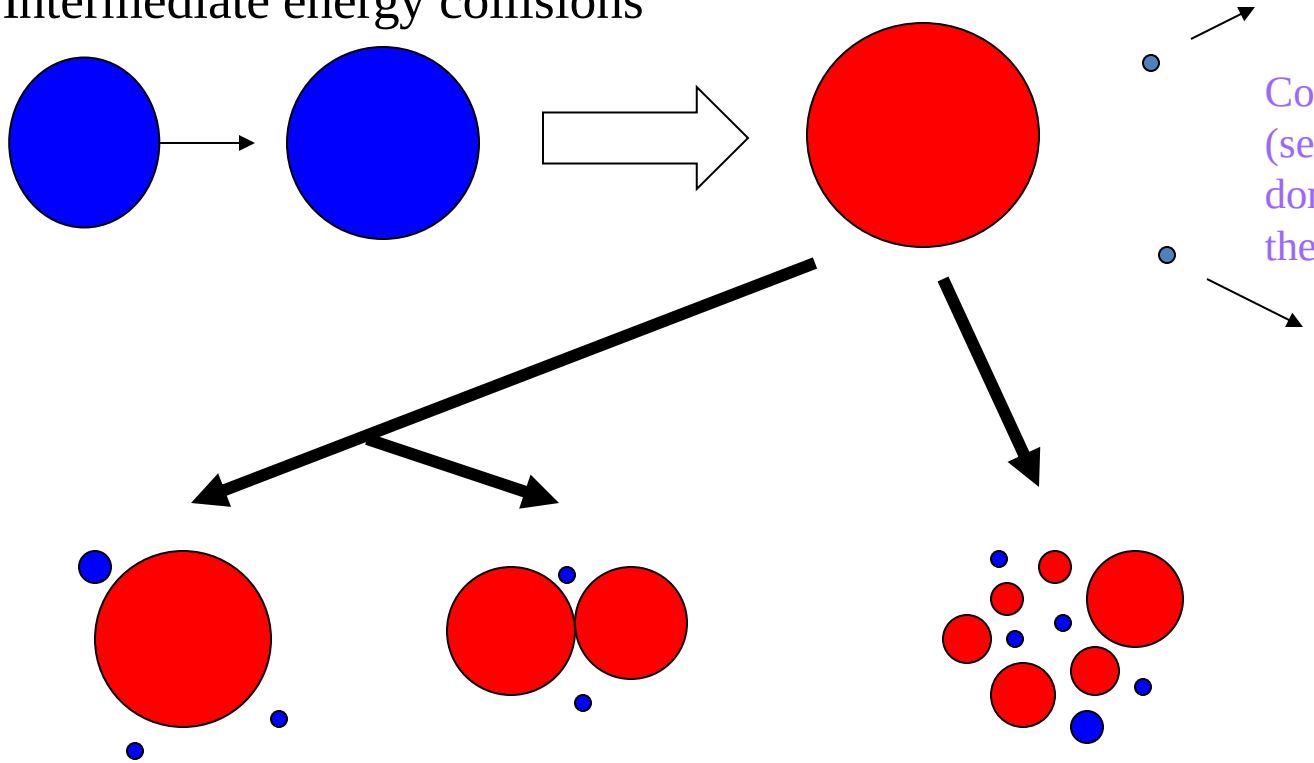

Compound-nucleus decay channels (sequential evaporation or fission) dominate at low excitation energy of thermal sources E^*<2-3 MeV/nucl.

At high excitation energy E^*>3-4 MeV/nucl there is a simultaneous break-up into many fragments

evaporation fission Multifragmentation

at freeze-out thermal and chemical equilibrium

Statistical Multifragmentation Model

[2] JP Bondorf, AS Botvina et al., Phys. Rep. 257, 133 1995.

Probability of channel: $W_f^{mic} = \frac{1}{\xi}\exp\{S_f(E_0, A, Z)\}, \quad \text{with} \quad \xi = \sum_f \exp\{S_f(E_0, A, Z)\}$

mass and charge conservation $\sum_{A,Z} N_{AZ}.A = A_0, \qquad \sum_{A,Z} N_{AZ}.Z = Z_0$

Energy conservation $E_0 = F_f - T_f \frac{\partial F_f}{\partial T_f}$

entropy of channel $S_f = -\frac{\partial F_f}{\partial T_f}$

Fragments obey Boltzmann statistics, liquid-drop description of individual fragments, Coulomb interaction in the Wigner-Seitz approximation

free energy of channel: $F_f = \sum_{A,Z} N_{AZ} F_{AZ} + \frac{3}{5}\frac{Z_0^2 e^2}{r_0 A_0^{1/3}(1+\chi_c)^{1/3}}$

Free energy of individual fragments: $F_{AZ} = F_{AZ}^b + F_{AZ}^s + F_{AZ}^{sym} + F_{AZ}^c$ liquid-drop model

Bulk term: $F_{AZ}^b = [-W_0 - T_f^2/\varepsilon_0(A)]A, \qquad W_0 = 16\ \text{MeV}$

Surface term: $F_{AZ}^s = B_0[(T_c^2 - T_f^2)/(T_c^2 + T_f^2)]^{5/4} A^{2/3}, \qquad B_0 = 18\ \text{MeV}$

Symmetry energy term: $F_{AZ}^{sym} = \gamma(N-Z)^2/A, \qquad T_c = 18\ \text{MeV}$

Coulomb term: $F_{AZ}^c = \frac{3}{5}\frac{Z_0^2 e^2}{r_0 A_0^{1/3}}[1-(1+\chi_c)^{-1/3}], \qquad \gamma = 25\ \text{MeV}$

MSU exp.: central collisions of $^{112,124}Sn+^{112,124}Sn$ at E/A= 50 MeV. (Liu TX *et al* 2004 *Phys. Rev.* C **69** 014603)

The microcanonical Markov-chain SMM calculations assuming the decay of single isolated source.

N Buyukcizmeci et al., J. Phys. G: Nucl. Part. Phys. 39 (2012) 115102

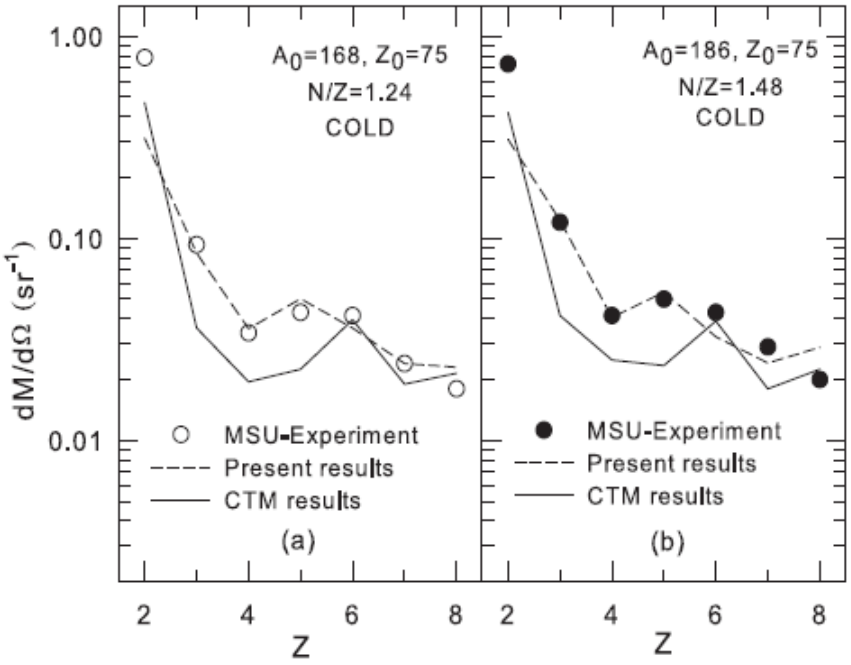

Predicted charge yields of light fragments (Z≤8) emitted from the multifragmentation of the sources, and the comparison with MSU experimental data.

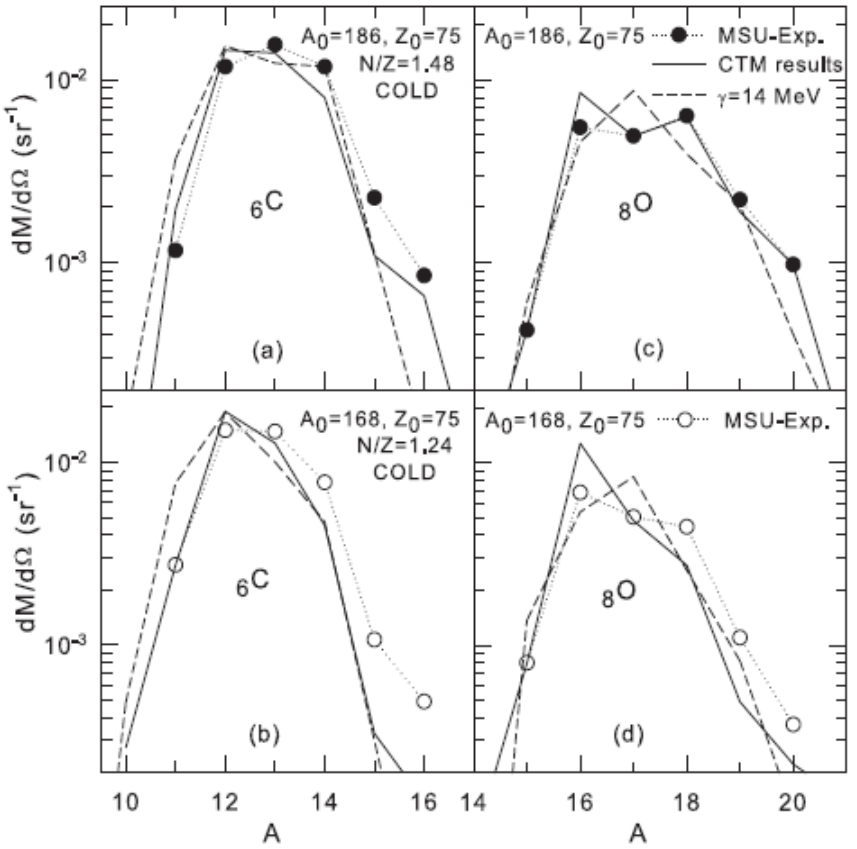

Predicted isotope distributions for carbon and oxygen fragments for the both sources. The panels (a) and (b) are for the carbon isotopes, and (c) and (d) for the oxygen isotopes. The dashed lines correspond to the present results for cold fragments at gamma=14 MeV, the circles to the MSU data, full lines CTM results.

ALADIN projectile fragmentation of ^{124}Sn, ^{107}Sn and ^{124}La beams at an incident energy of 600 MeV per nucleon studied with ALADIN spectrometer.

Isotope distributions: comparison S254 data-SMM calculations

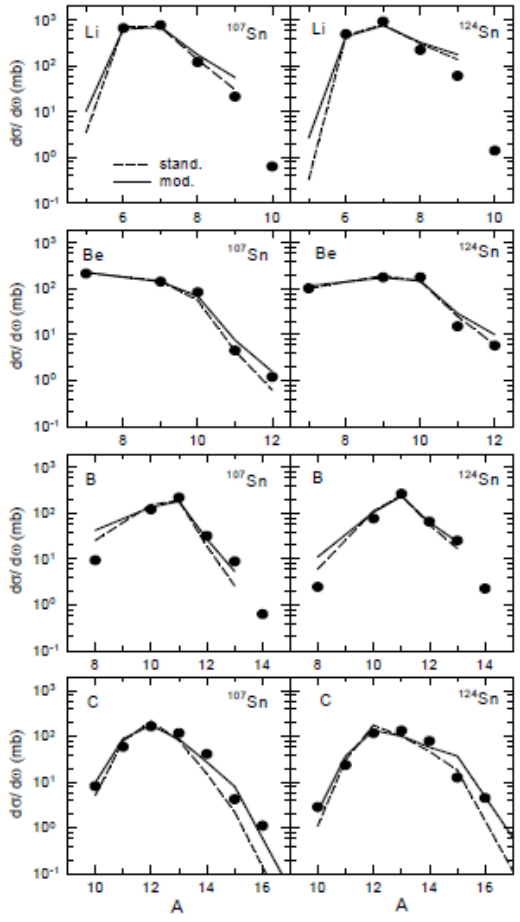

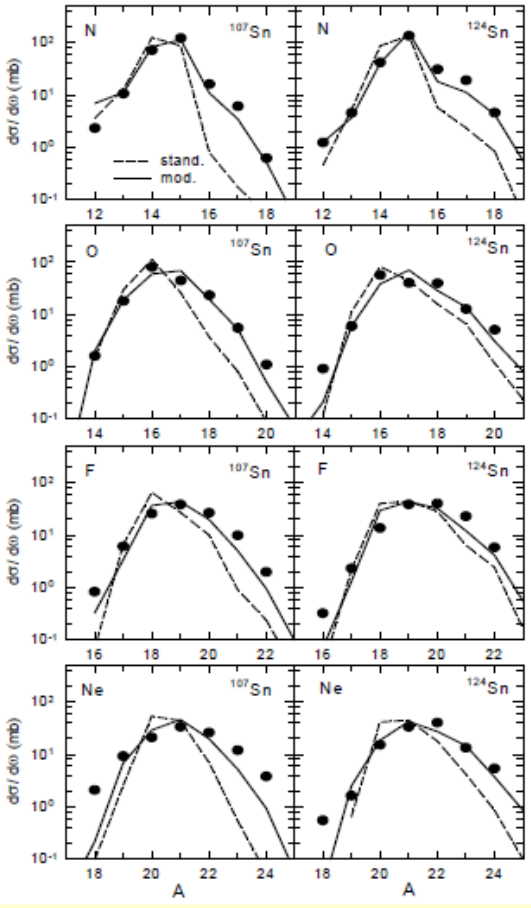

Z=3-10

B_0=19 MeV for ^{107}Sn

B_0=17.5 MeV for ^{124}Sn

ensemble parameter
a_2=0.015 MeV^{-2}

Z_{bound}/Z_0=0.2-0.8

Solid lines
γ=14 MeV

Dashed lines
γ=25 MeV

SMM Ensemble Calculations

R. Ogul, A.S. Botvina , Atav U., Buyukcizmeci N. ,et al., Phys. Rev. C 83, 024608 (2011).
J. P. Bondorf et al., *Phys. Rep.* 257, 133 (1995).
N. Buyukcizmeci, R. Ogul, A.S. Botvina, *Eur. Phys. J. A* 25 57 (2005).

Comparing our results with ALADIN S254 data, it is confirmed that a significant reduction of symmetry energy term γ is found necessary to reproduce <N>/Z of Z ≤ 10 fragments. The symmetry energy of these fragments are considerably reduced in multifragmentation region, in comparison with the cold isolated fragments.

FRS data @ GSI

FRS projectile fragmentation of two symetric systems ^{124}Sn + ^{124}Sn and ^{112}Sn + ^{112}Sn at an incident beam energy of 1 A GeV measured with high-resolution magnetic spectrometer FRS.
(V. Föhr, et al., Phys. Rev. **C 84**, (2011) 054605)

Experimental data are well reproduced with statistical calculations in the SMM–ensemble .
To reproduce the FRS data symmetry energy term is reduced as shown in the table.
We have also found a decreasing trend of the symmetry energy with increasing charge number, for the neutron-rich heavy fragments resulting from 124Sn projectile.
H. Imal, A.Ergun, N. Buyukcizmeci, R.Ogul, A.S. Botvina, W. Trautmann, C **91**, 034605 (2015)

Symmetry-energy coefficients.

Z interval	^{112}Sn γ(MeV)	^{124}Sn γ (MeV)
10-17	16	16
18-25	19	18
26-31	21	20
32-37	23	19
38-45	25	18

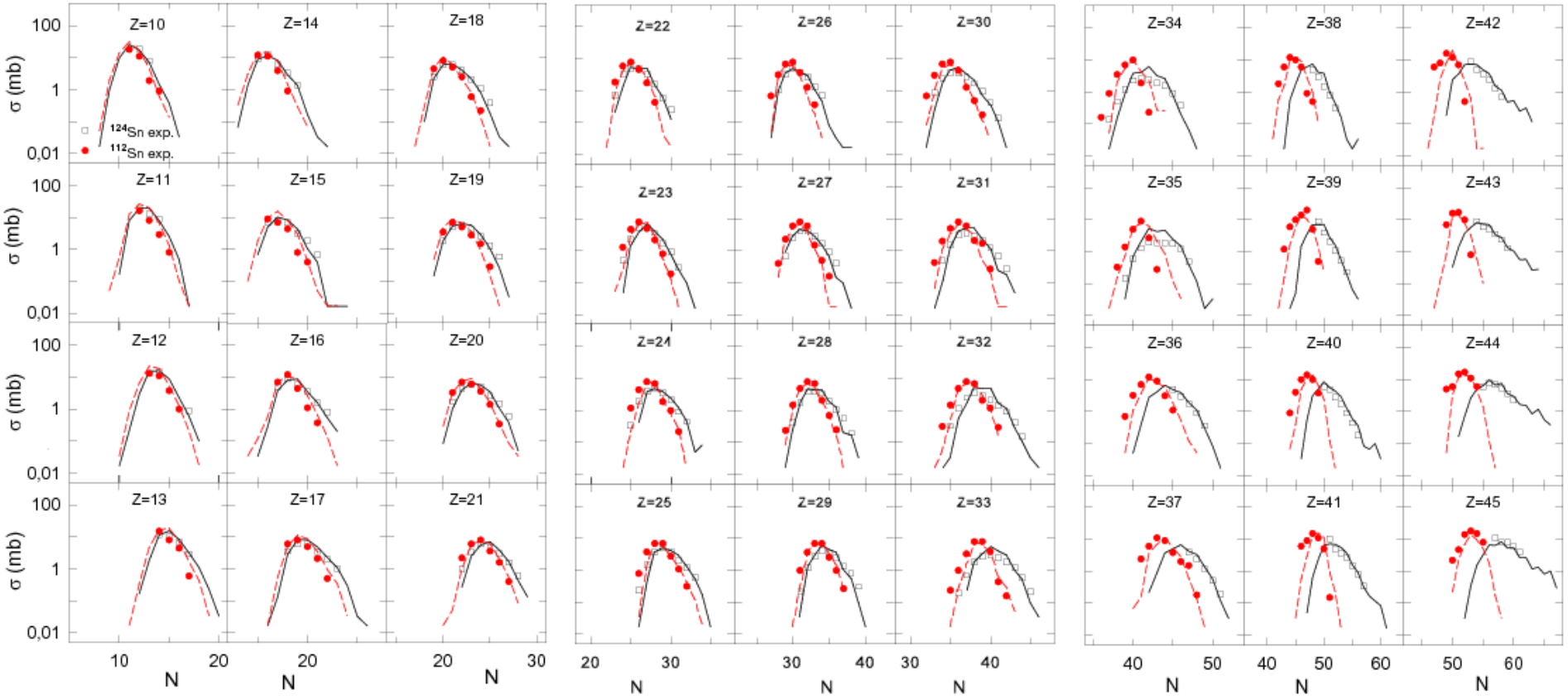

Angular momentum and Coulomb effects for hot fragments in peripheral HICs at Fermi energies

peripheral ^{84}Kr+^{84}Kr collisions at energy of 35 MeV per nucleon

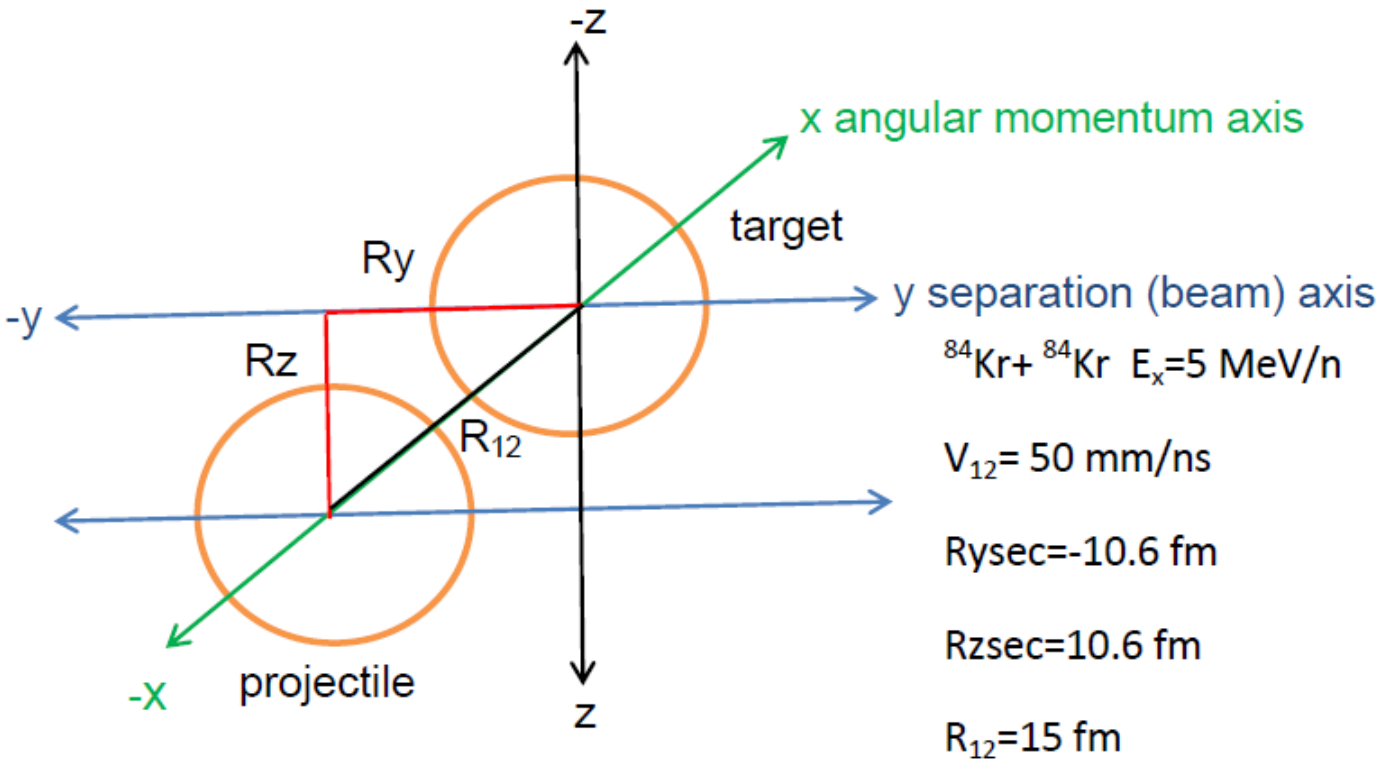

The first source (projectile) is flying along Y -axis.

The location of the second (target) source is RY =-10.6 fm and RZ=10.6 fm respective to the first source.

The peripheral collision is assumed to take place in the Y-Z plane, therefore, the coordinate in Z-axis is determined by the sizes of colliding nuclei, as well as their possible repulsion after the collision.

The X-axis is assumed to be an angular momentum axis.

Charge distribution

A.Ergun, H. Imal, N. Buyukcizmeci, R. Ogul, A.S. Botvina, Phys. Rev. C **92**, 014610 (2015)

$\rho=\rho_0/2$

$\rho=\rho_0/6$

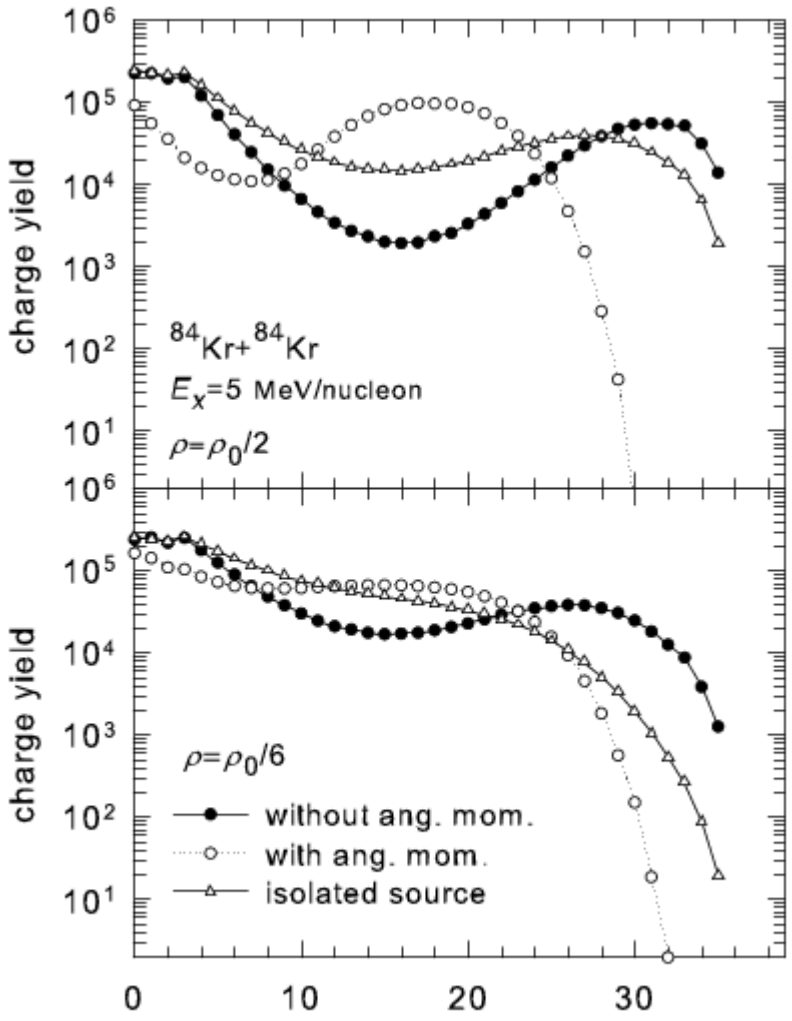

Fig.1: Total charge yield of primary hot fragments, in the cases of without (full circles) and with angular momentum (L) of 80ħ (open circles), after multifragmentation of the ^{84}Kr source at the excitation energy of Ex = 5 MeV/nucleon.

This projectile source is assumed to be formed in the peripheral ^{84}Kr+^{84}Kr collision at 35 MeV/nucleon, and its disintegration are affected by the Coulomb field of the partner. Top and bottom panels show results at freeze-out densities ρ= ρ0/2, and ρ=ρ0/6, respectively.

For comparison, the results of multifragmentation of a single isolated ^{84}Kr source, at the same excitation energy but without the external Coulomb and without angular momentum, is shown too.

An angular momentum (open circles) favors emission of IMF(Z=3-20) with larger charge (mass) numbers since the system in the freeze-out needs to have a large moment of inertia in order to minimize rotational energy and maximize the entropy. From another side a Coulomb interaction (full circles) prevents to emit IMF with large charge number Z.

Charge distribution of the first, second and third largest hot fragments

A.Ergun, H. Imal, N. Buyukcizmeci, R. Ogul, A.S. Botvina, Phys. Rev. C **92**, 014610 (2015)

$\rho=\rho_0/2$ $\rho=\rho_0/6$

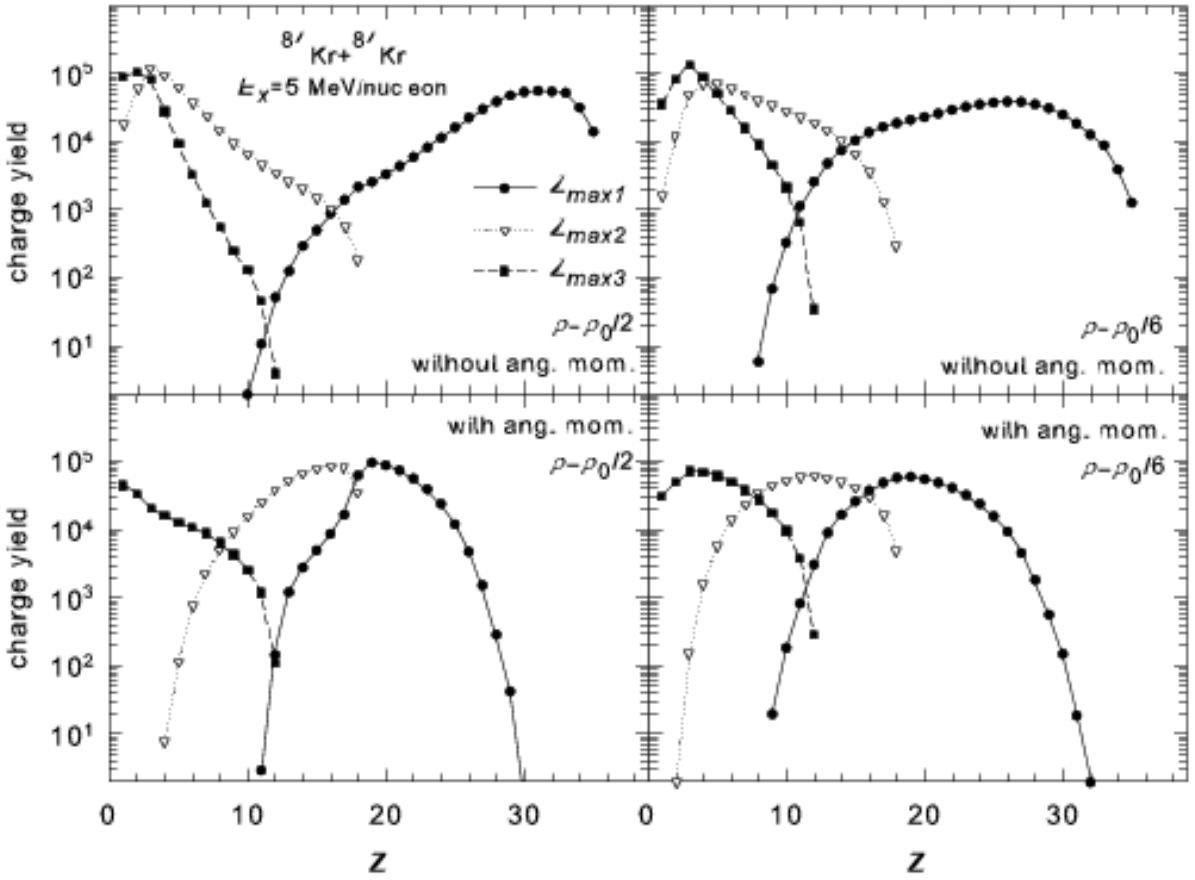

L= $0\hbar$
only Coulomb effect

L= $80\hbar$ angular momentum
+ Coulomb effect

Fig. 2: The yields of the first, second and third largest hot fragments with the atomic numbers Z_{max1}, Z_{max2}, and Z_{max3}, respectively, for ^{84}Kr+^{84}Kr reaction at E_x=5 MeV/n.

<N>/Z distributions

The angular momentum leads to increasing N/Z values of IMFs

^{84}Kr : initial <N>/Z=1.33

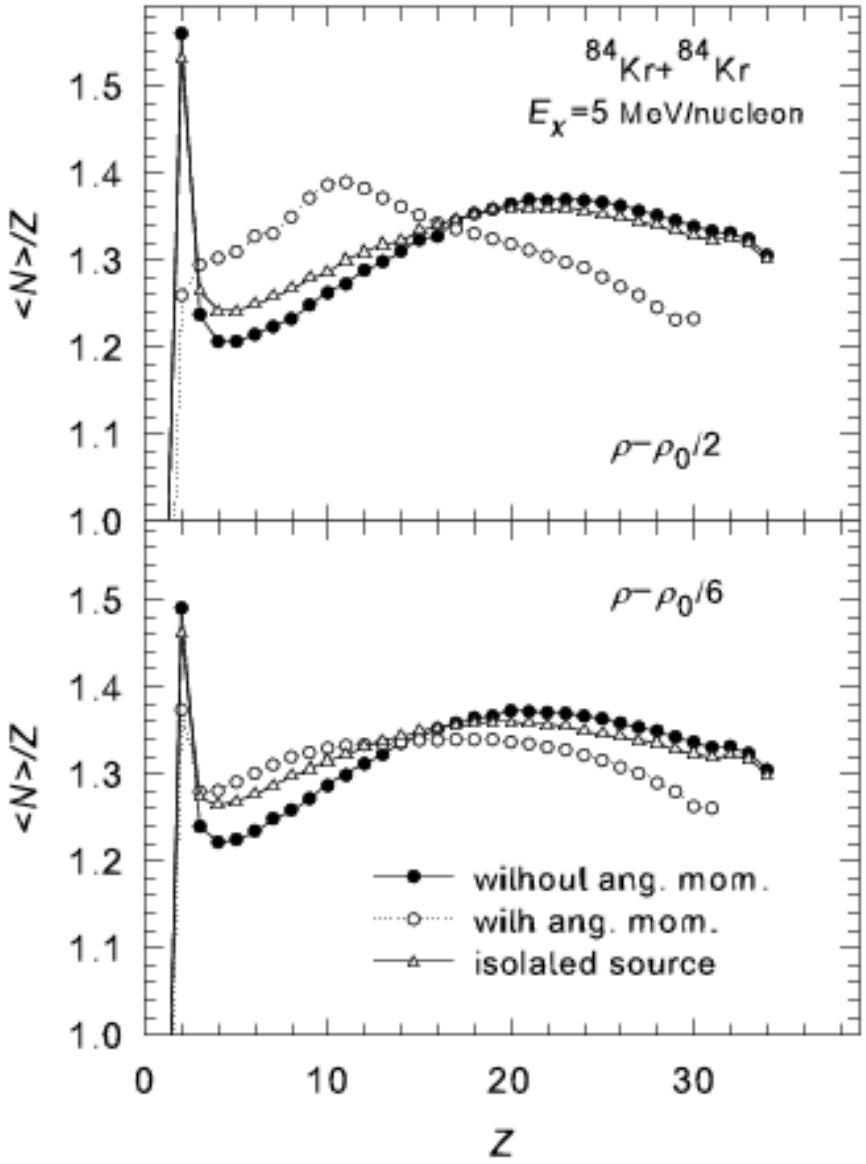

Fig.3 :The average neutron-to-proton ratio <N> /Z of hot primary fragments produced in the freeze-out $\rho = \rho 0/2$ (top panel) and $\rho = \rho 0/6$ (bottom panel) for 84Kr+84Kr at Ex=5 MeV/n. Full and empty circles show the distributions in the case of L=0 hbar and including angular momentum L=80 hbar, respectively.

Theoretical Calculation of V_x And V_y Velocity Distributions for $^{84}Kr+^{84}Kr$

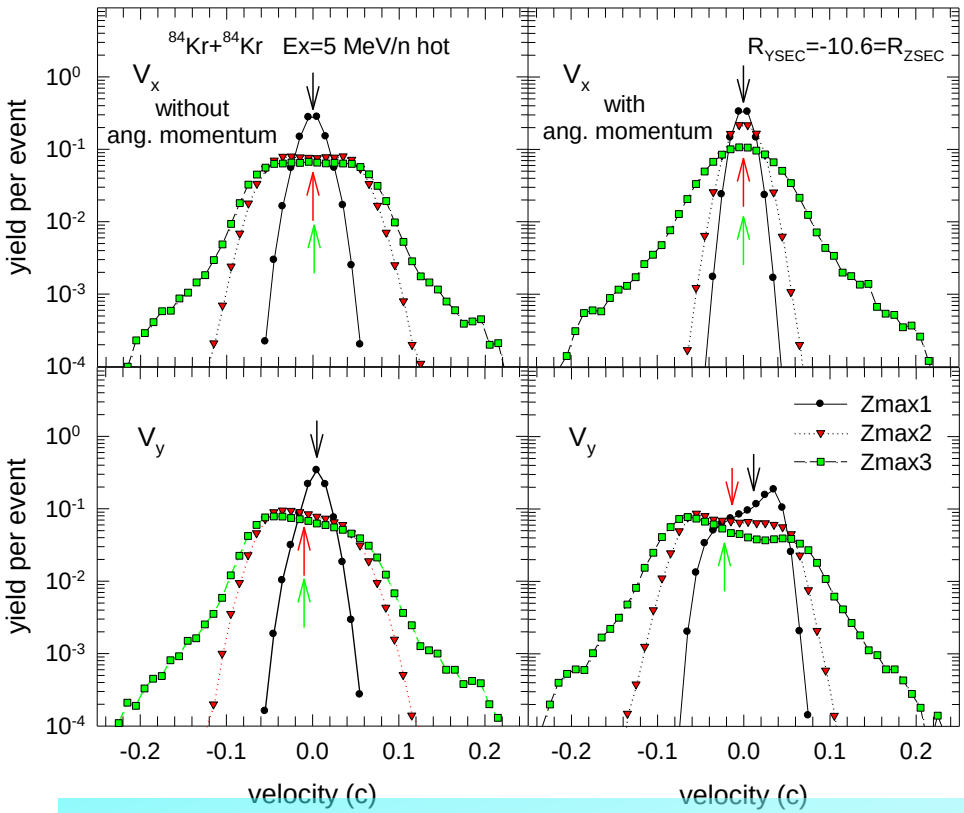

Calculations are done over 100.000 events for this fig.

➡ X – angular momentum direction

➡ Y – reaction direction

Figure 4: Theoretical calculations of V_x and V_y velocity distributions of 1_{st}, 2_{nd} and 3_{rd} charged hot particles without (left) and with (right) inclusion of angular momentum for $^{84}Kr+^{84}Kr$ reaction at E_x=5 MeV/n.

In the case of inclusion of angular momentum, all these fragments fly predominantly in the plane of rotation. This is seen from the peaked distributions at V_x.

As a result of Coulomb proximity, the maximum fragments fly predominantly in forward direction, while second and third ones fly in the direction of the target sources.

There is an order in emission of these fragments: The largest fragments have the largest V_y velocity, and then 2_{nd} and 3_{rd} ones (As is seen from V_y panel). This effect is consistent with the previous experimental observations [J. Colin et al., *Phys. Rev. C* 67, 064603 (2003).]

<N/Z> and yield per event for velocity distribution Vy

Z=3, 6, 9, 12, 15, 18

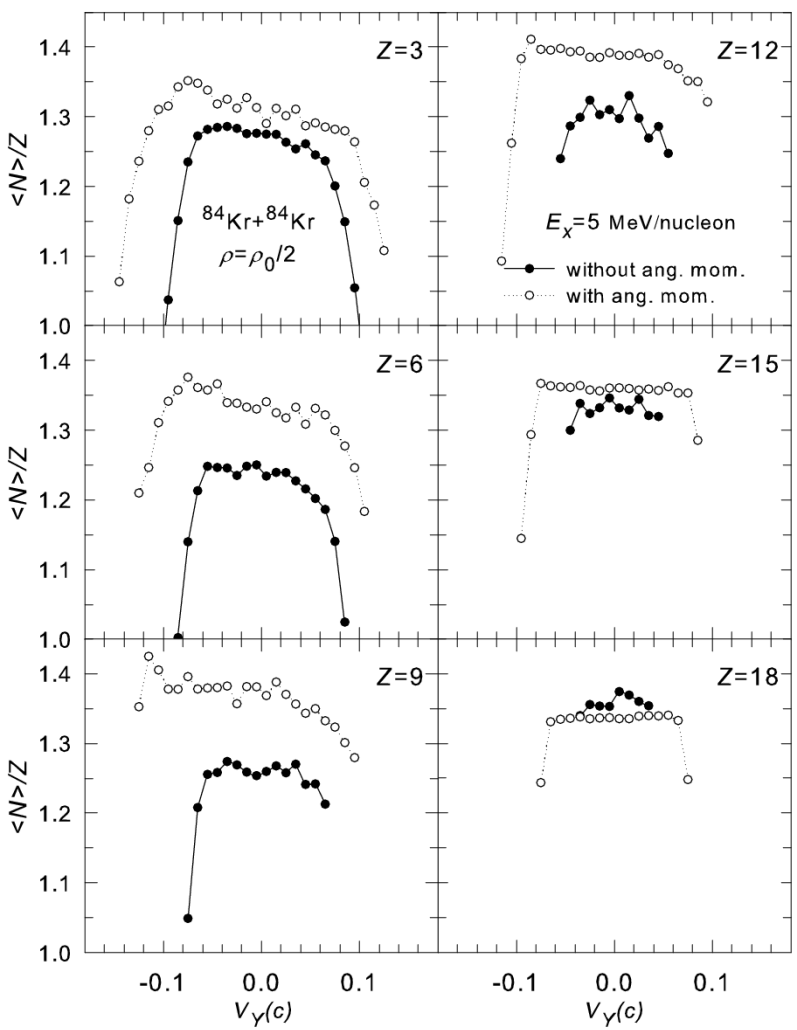

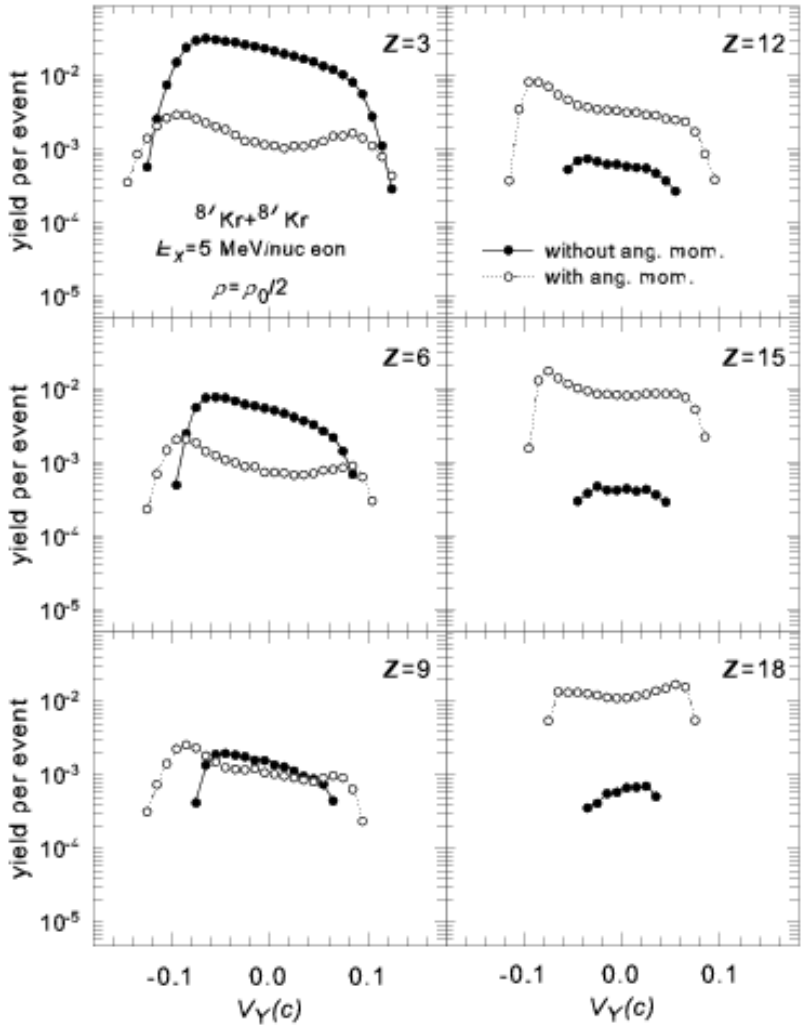

Figure 5-6 : < N > /Z and yield per event as a function of velocity Vy. Full and open circles show the distributions for L = 0$\hbar$ and L = 80$\hbar$, respectively.

<Z> and <N>/Z vs velocity Vy

L = 0$\hbar$ L= 80$\hbar$

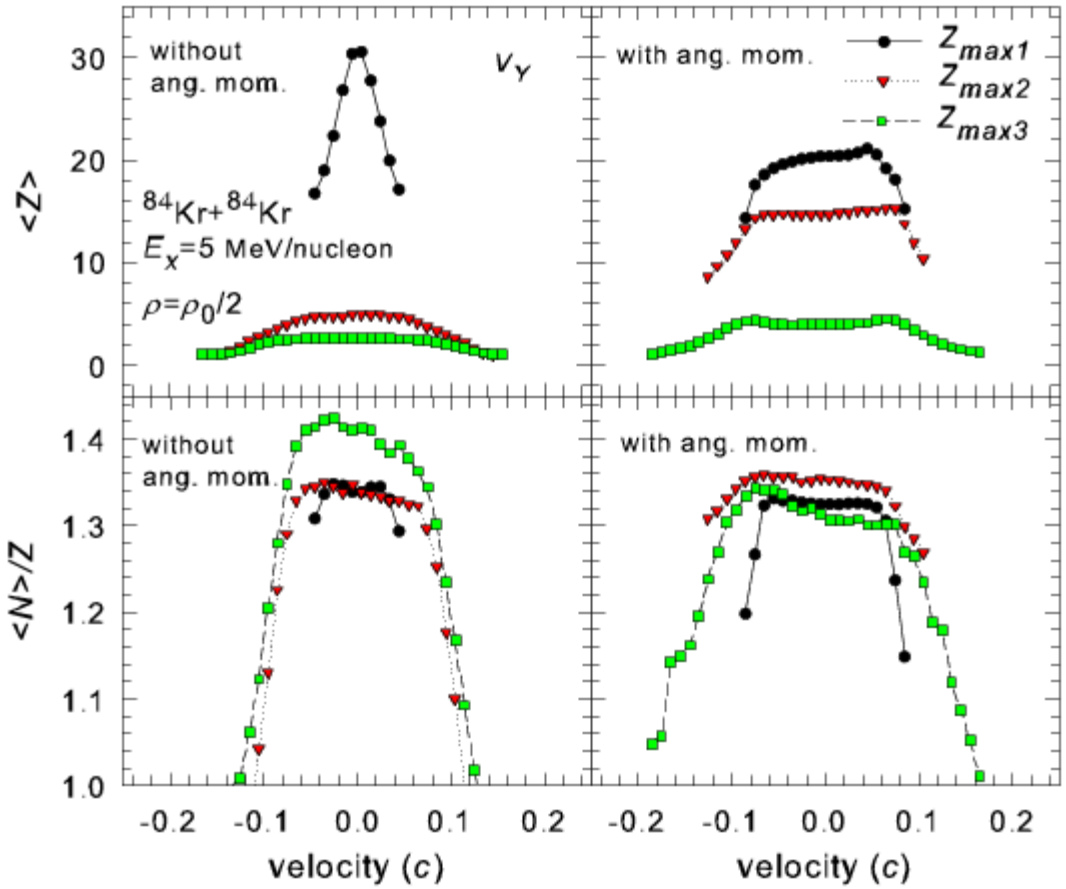

Fig.7: Average charge <Z> (top) and <N>/Z (bottom) distributions of the first, second and third largest hot fragments with the atomic numbers Z_{max1}, Z_{max2}, and Z_{max3}, respectively, according to the V_y for hot primary fragments produced in the freeze-out density $\rho=\rho_0/2$ for $^{84}Kr+^{84}Kr$ at E_x=5 MeV/n.

It is in agreement with our previous conclusions on modification of statistical picture. In particular, one can see a trend of increasing < N > /Z toward midrapidity for Z_{max3} when the angular momentum is included (right bottom panel).

Dependence of the fragment characteristics on distances between the sources

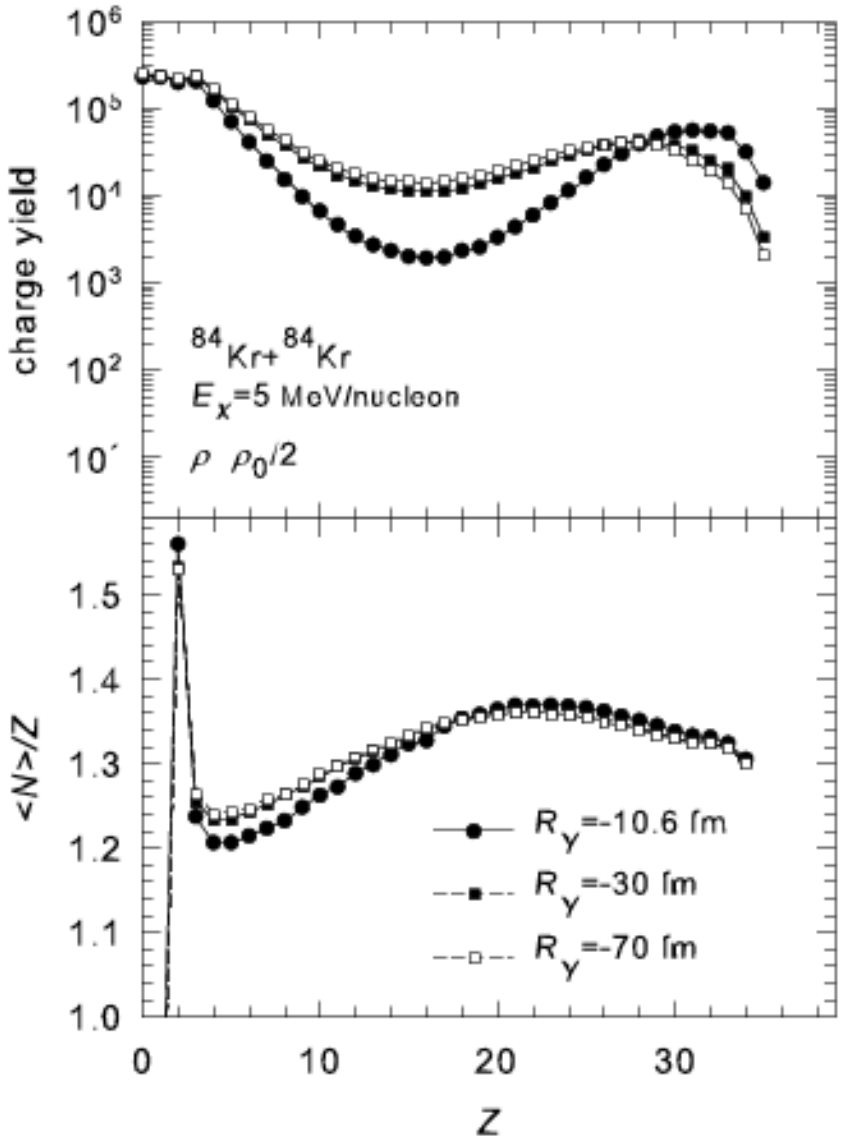

Fig.8:The total charge yield (top panel) and the mean neutron-to-proton ratios $<N>/Z$ (bottom panel) of all primary fragments produced at the freeze-out density $\rho=\rho_0/2$ for ^{84}Kr+^{84}Kr at E_x=5 MeV/n., and at different distances between the sources

To clarify the Coulomb contribution, we do not include the angular momentum here.

If Ry=-70 fm:
The decrease of the external Coulomb field leads to the enhanced IMF production because of a lower Coulomb barrier. The expected distributions are very close to those obtained in the case of isolated sources

The neutron richness of these fragments increases slightly and, correspondingly, the neutron content of the largest fragment decreases, in correlation with their more uniform distribution in the coordinate space.

Dependence of the fragment characteristics on distances between the sources: yields and <N>/Z vs velocity Vy

A.Ergun, H. Imal, N. Buyukcizmeci, R. Ogul, A.S. Botvina, Phys. Rev. C **92**, 014610 (2015)

Double nuclear system

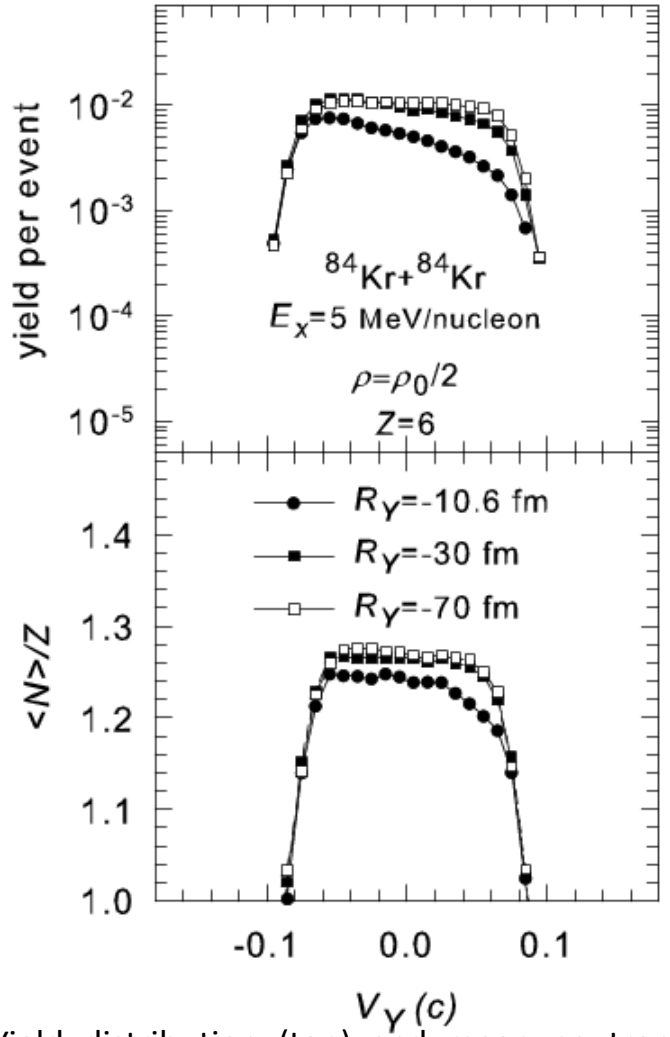

Fig.9:Yield distribution (top) and mean neutron-to-proton ratios <*N*>/*Z* (bottom) of primary fragments with *Z*=6 as a function of their velocity *VY* in the source frame, at different distances between the sources.

Double nuclear system+necklike fragment (C)

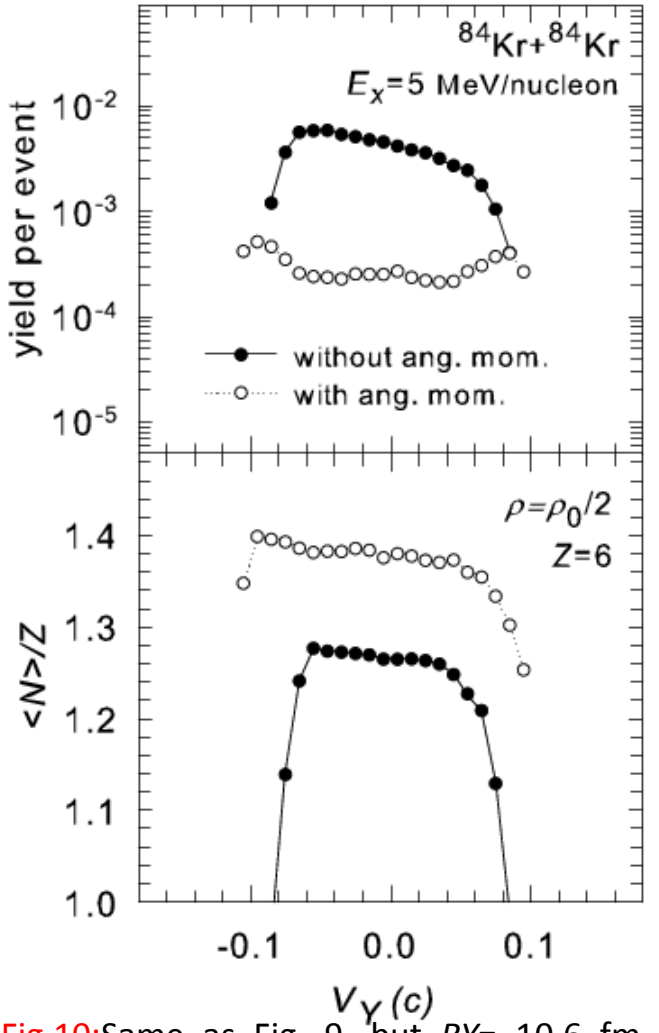

Fig.10:Same as Fig. 9, but *RY*=−10.6 fm between the sources and with the presence of the neck-like fragment (*A* = 12, *Z* = 6) at midrapidity between the sources. *L* = 80 hbar

3.Theoretical interpretation of FAZIA[1] $^{84}Kr+^{112,124}Sn$ reactions at an incident beam energy of 35 MeV/n including the Coulomb proximity and angular momentum effects on multifragmentation picture with Markov chain SMM .

[1]. S. Barlini, S. Piantelli, et al., Phys. Rev. C 87, (2013) 054607.

the correlation between excitation energy and velocity of projectile residues for $^{84}Kr + ^{112,124}Sn$

Ex (MeV/n)	Zs	As(112Sn)	As(124Sn)	Vs(112Sn) (mm/ns)	Vs(124Sn) (mm/ns)	Weight	Angular Momentum (h-bars)
2	34	77	82	71.498	71.043	0.13	30
3	33	75	80	68.082	67.703	0.19	30
4	32	73	77	64.515	63.756	0.32	40
5	30	68	73	60.264	58.898	0.25	40
6	29	66	70	54.799	53.129	0.08	40
7	28	64	68	46.980	44.931	0.03	40

Table 1. Values used for SMM calculations as initial parameters. Vlab=Vs+Vcm
While the less excited (Ex=2 MeV/n) projectile sources fly more quickly, the highly excited (Ex=7 MeV/n) projectile sources fly more slowly.

We have found velocity of sources from energy and momentum conservation.

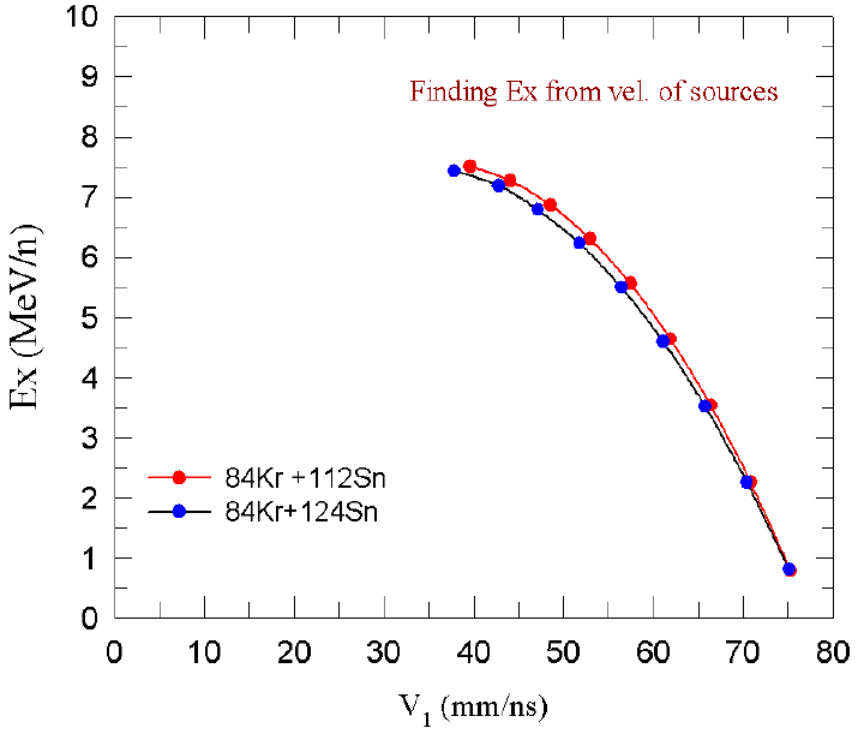

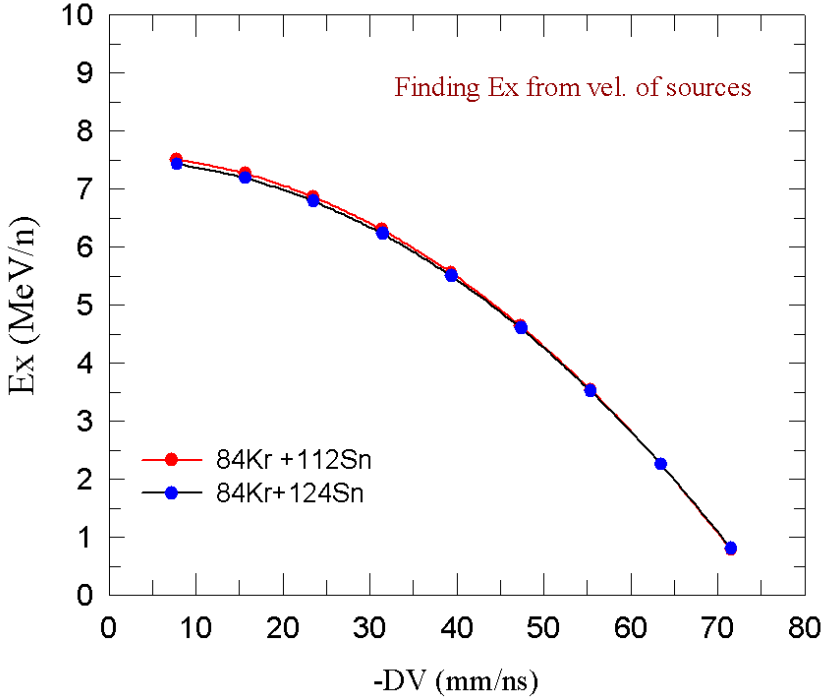

V1 velocity of projectile

V2 velocity of target

Velocity of target in projectile system DV=V2-V1

Fig 6: Ex excitation energy vs average velocities of projectile residues for ^{84}Kr + ^{112,124}Sn. kinetic energy of the projectile : 35 MeV/n

Charge distributions : FAZIA [1] data-SMM calculations

Inclusive charge distribution of fragments (Z≥ 3) produced in the ^{84}Kr+^{112}Sn *(red solid dots)* and ^{84}Kr+^{124}Sn *(black open dots) reactions at 35 MeV/n. The distributions are normalized in the region 18≤Z≤28.* [1] S. Barlini et al., Phys. Rev. C 87, (2013) 054607. *We have ignored Ex<2 MeV/n cases in SMM calculations. Trends seems similar.*

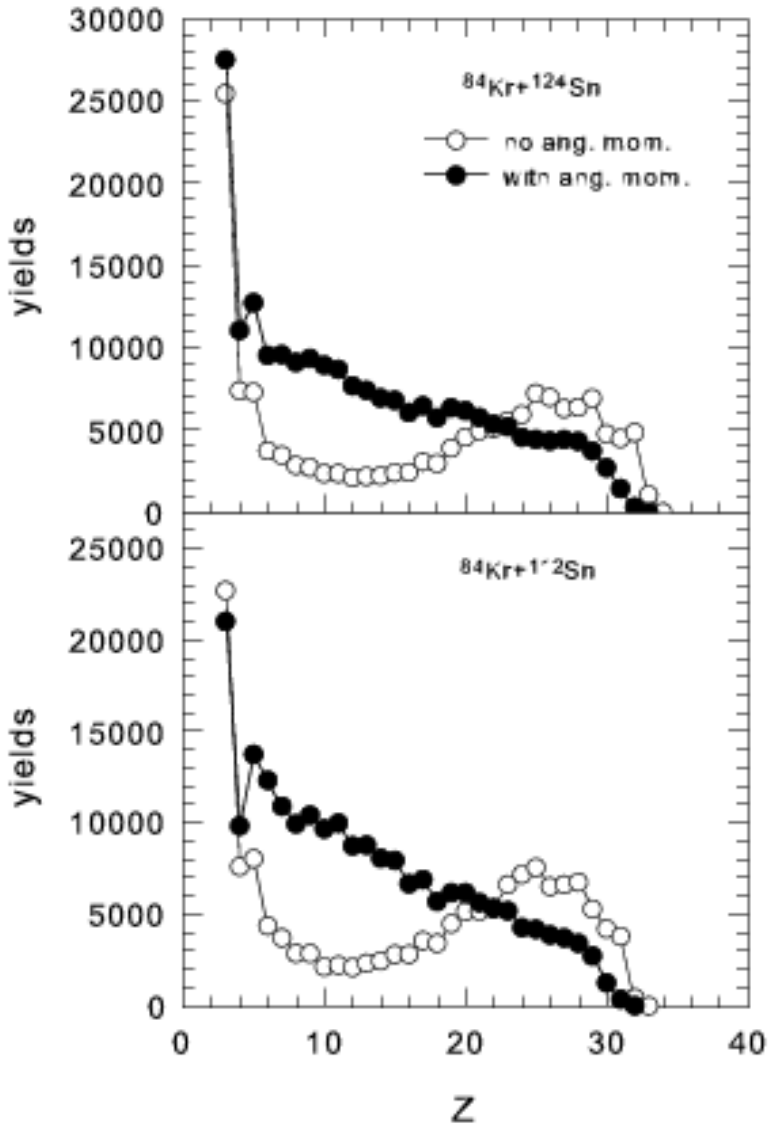

(preliminary results)

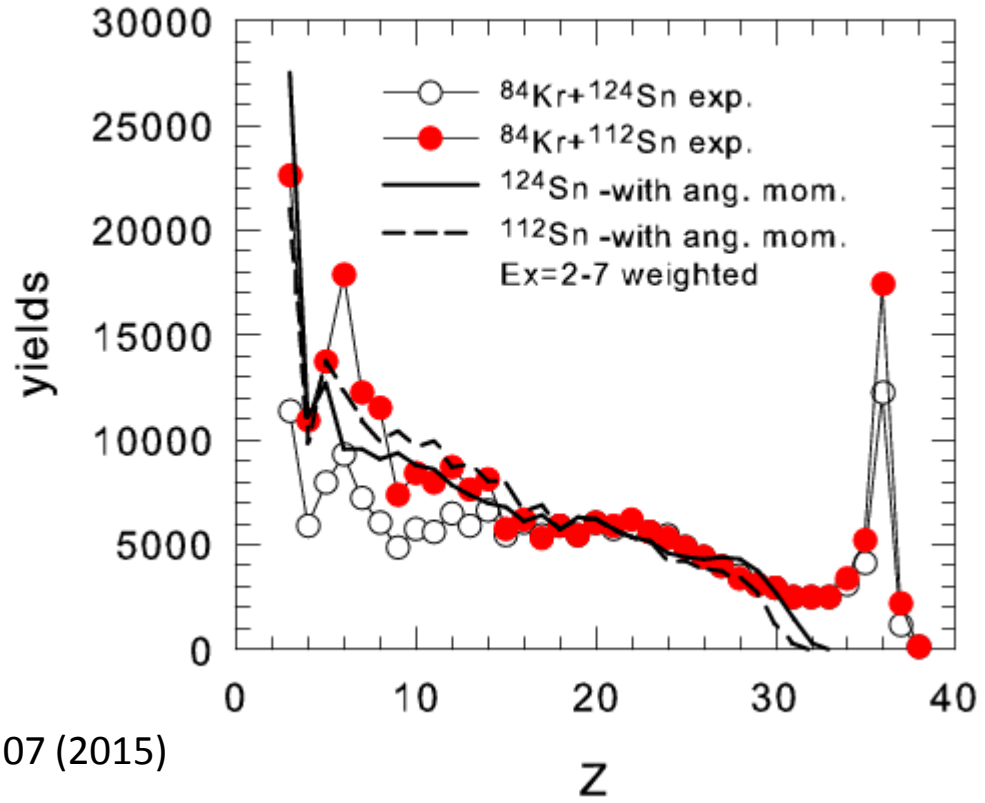

Buyukcizmeci et al. Nuc. Sci. And Tech. 26, S20507 (2015)

<N>/Z Distributions: FAZIA[1] data-SMM calculations

The <N>/Z of the products detected in the n-rich case is systematically higher than the <N>/Z of the n-poor case.

without angular momentum

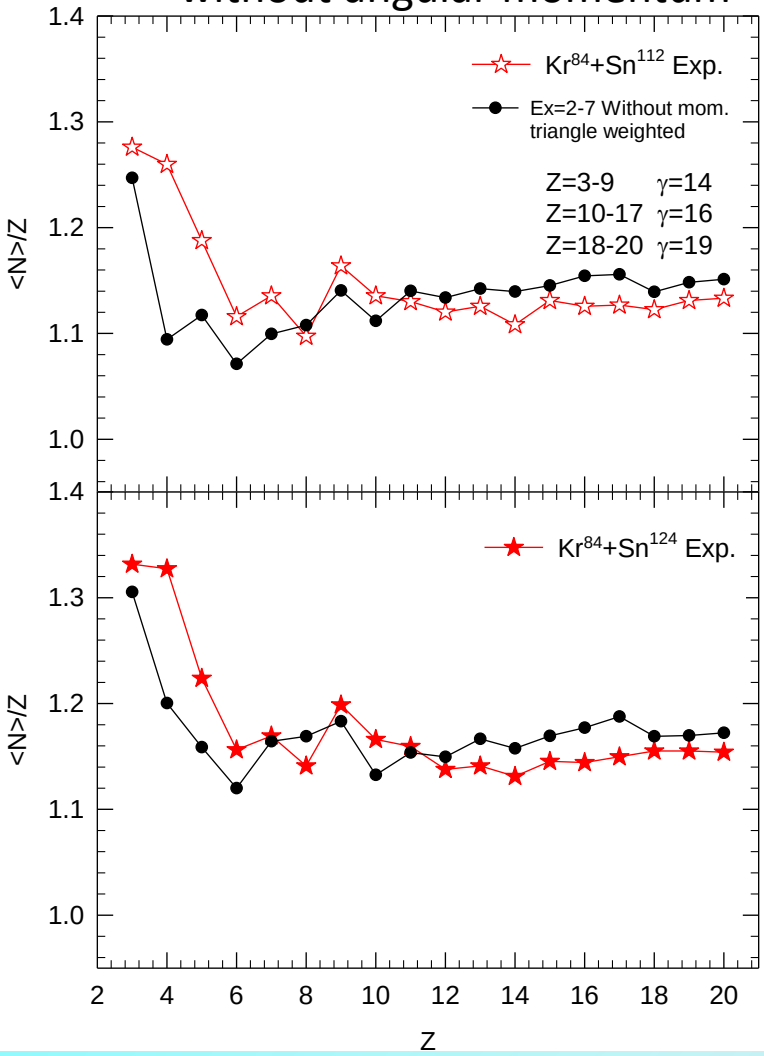

with angular momentum

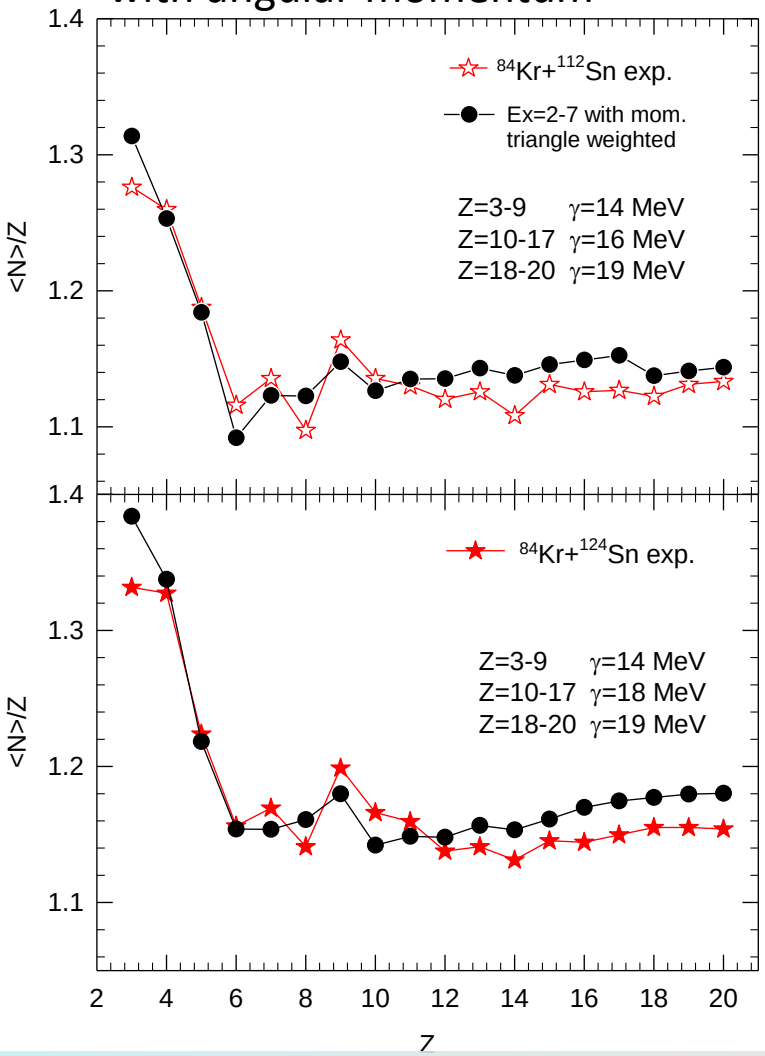

Şekil 8: <*N*>/*Z* as a function of *Z* for the reaction ^{84}Kr+^{124}Sn (red full stars) and ^{84}Kr+^{112}Sn (red open stars) at 35 MeV/nucleon [1].

Isotopic Distributions: SMM calculations

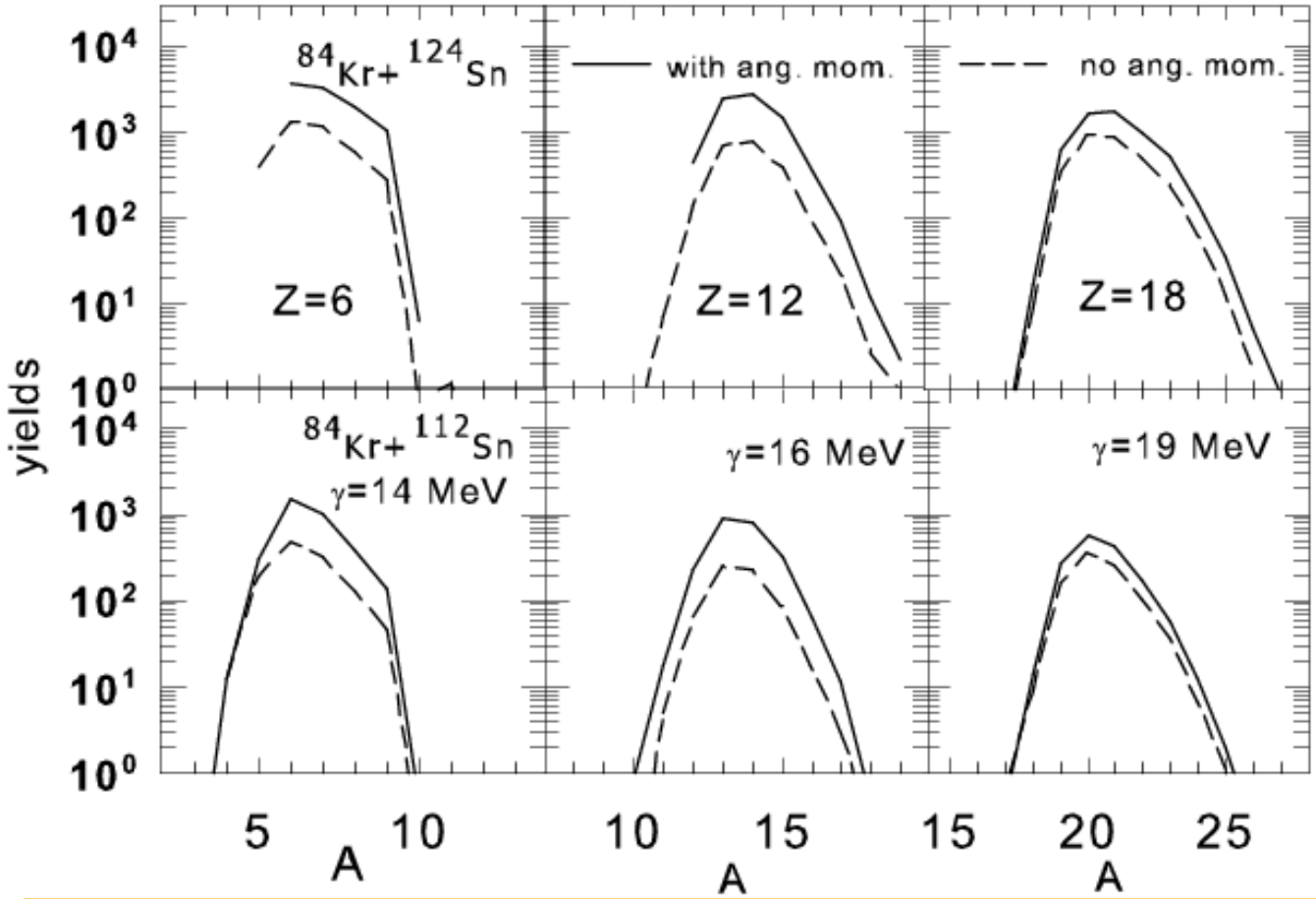

Z=3-9 γ=14 MeV
Z=10-17 γ=16 MeV
Z=18-20 γ=19 MeV

Fig . Predicted isotope distributions for Z =6, 12, 18 fragments for ^{84}Kr+^{124}Sn (top panels) and ^{84}Kr+^{124}Sn (bottom panels) reactions. The solid lines correspond to the present results with angular momentum, the dashed lines show results without angular momentum. For our predictions γ =14, 16 and 19 MeV values are used for Z=6, 12 and 18 isotopes, respectively. These γ values are in agreement with our previous predictions in [13].

Isotopic Distributions: Comparison FAZIA data-SMM calculations

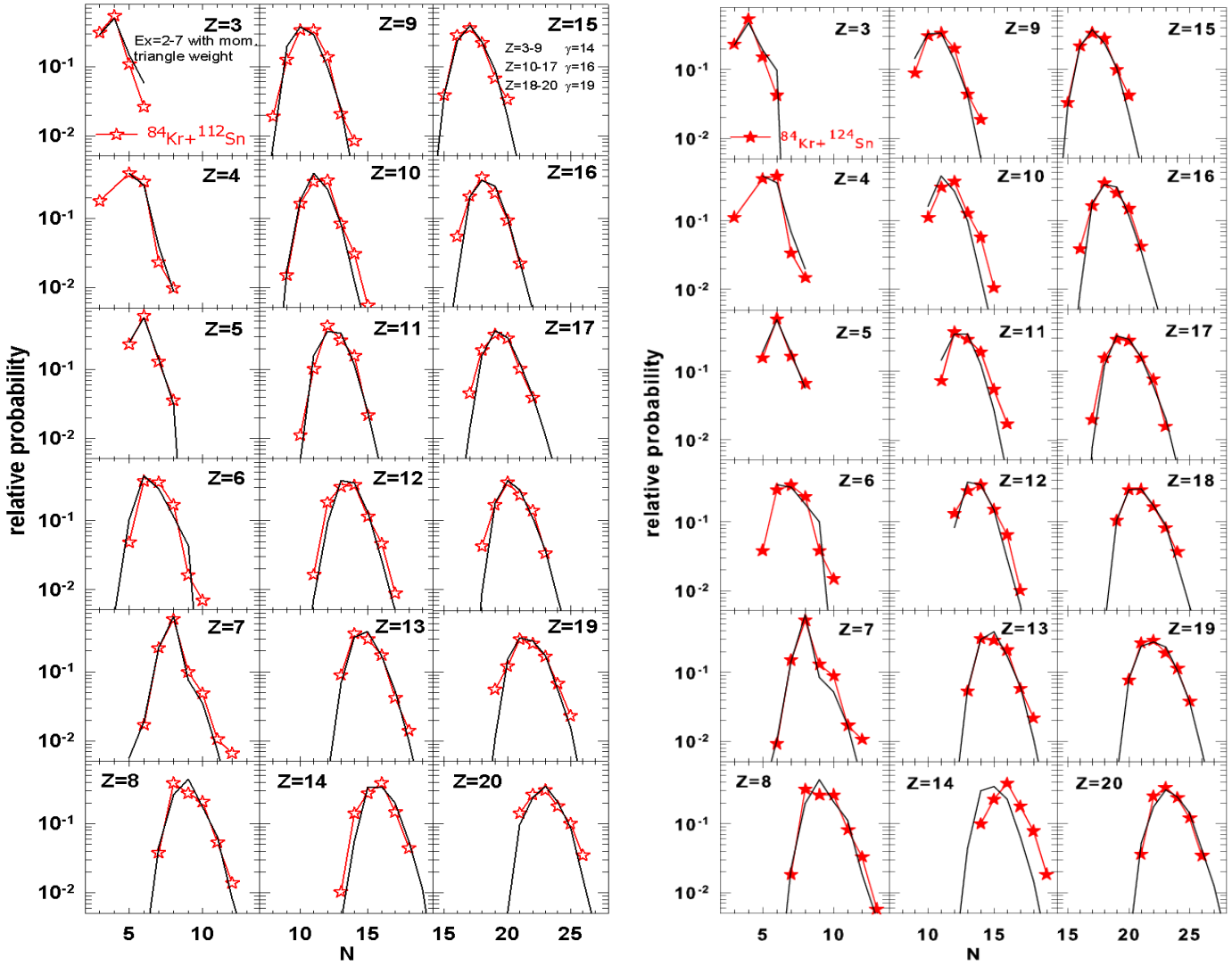

Z=3-9 γ=14 MeV
Z=10-17 γ=16 MeV
Z=18-20 γ=19 MeV

Fig . Predicted isotope distributions for Z = 3–20 fragments for ^{84}Kr+^{112}Sn (left panels) and ^{84}Kr+^{124}Sn (right panels) reactions. The solid lines correspond to the present results and the stars to the FAZIA data [1].

Angular momentum effect is very important to describe the velocities of fragments.

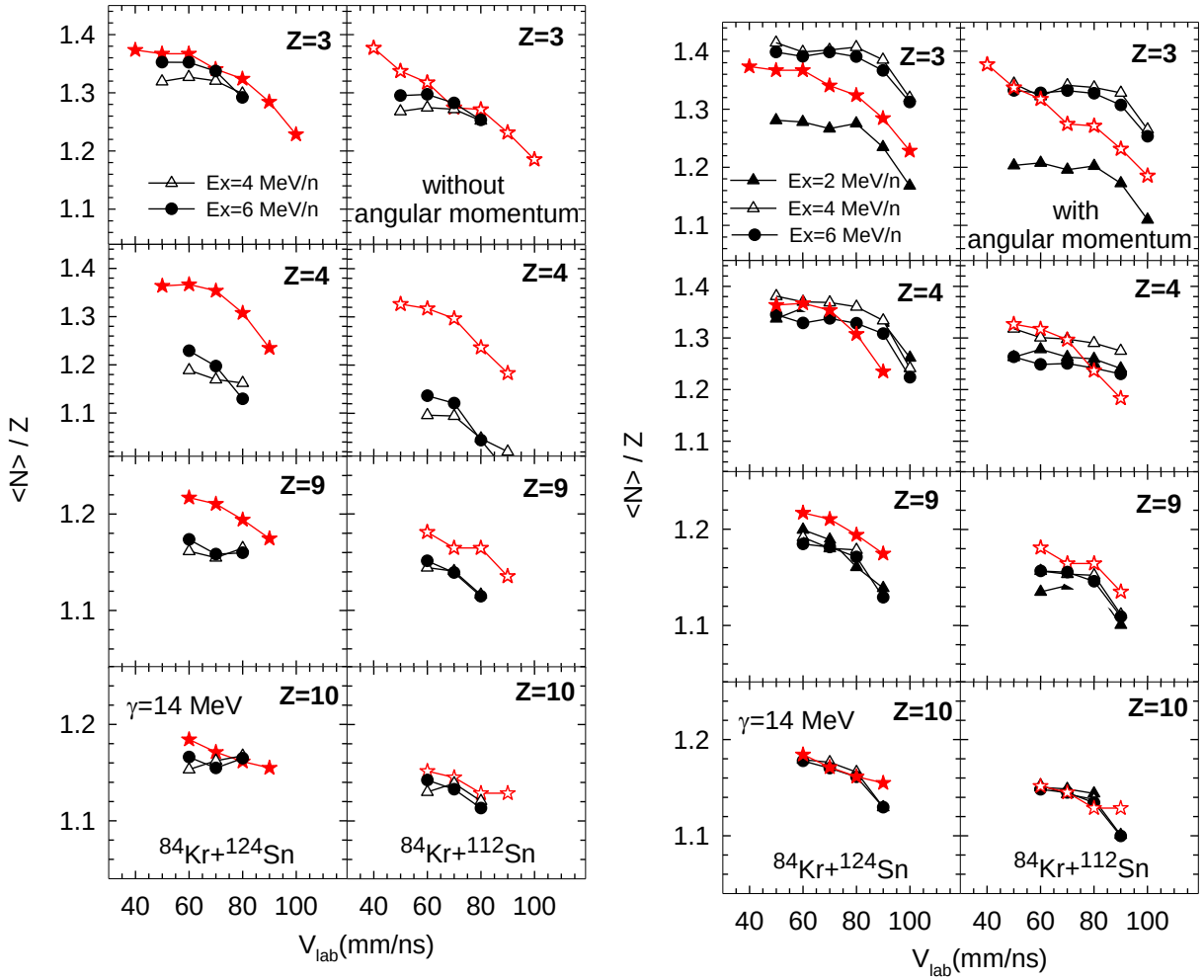

Figure 4: The evolution of <N>/Z for elements (Z=3, 4, 9, 10) as a function of the laboratory velocity of the fragments for $^{84}Kr+^{112}Sn$ (open stars) and $^{84}Kr+^{124}Sn$ (full stars) reactions [1]. SMM calculations without (left figures) and with (right figures) the inclusion of angular momentum of sources (see Table 1) for γ=14 MeV are shown.

- The less excited (Ex=2 MeV/n) projectile sources fly more quickly and produces not very neutron rich light fragments.
- While more excited sources (Ex=4-6 MeV/n) fly slower, and as a result of their decay more neutron rich light fragments are produced.
- We observe a clear increasing <N>/Z of these fragments toward midrapidity.
- During the evolution of <N>/Z, n-rich system are always above n-poor system.
- For light ions <N>/Z rapidly decreases with increasing velocity, while it displays a rather flat behavior for heavier ions.

CONCLUSIONS

These are our preliminary results.

Investigation of the influence of angular momentum and Coulomb proximity on fragment production in heavy-ion collisions at Fermi energies, including the description of FAZIA [1] experimental data, within the statistical approaches [5-13] is very promising.

Including an angular momentum and a long-range Coulomb interaction between projectile and target residues leads to new features in the statistical fragmentation picture: It is possible to obtain a correlation of sizes of emited fragments with their velocities and an emission in the reaction plane. [11]

The angular momentum may lead to more neutron-rich IMF production and to anisotropic emission respective to the projectile and target sources.

Coulomb interaction of the target and projectile-like sources leads to a predominant midrapidity (”neck”-like) emission of intermediate mass fragments.

We see a significant influence of these effects on the isotope production both in the midrapidity and in the kinematic regions of the projectile/target.

This kind of investigations may provide us with inputs to understand the nuclear equation of state and nuclear composition, which are important to determine the properties of nuclear and stellar matter at extreme conditions and their connections to the thermodynamics of stellar matter and astrophysical events.

REFERENCES

[1] S. Barlini et al., Phys. Rev. C 87, (2013) 054607.

[2] J. P. Bondorf et al., *Phys. Rep.* 257, 133 (1995).

[3]A.S. Botvina, I.N. Mishustin, *Phys. Rev. C* 63, 061601(R) (2001).

[4] A.S. Botvina, *arXiV:nucl-th/0008068* , (2000).

[5] N. Buyukcizmeci, H. Imal, R. Ogul, A.S. Botvina and I.N. Mishustin, J. Phys. G: Nucl. Part. Phys. 39 (2012) 115102.

[6] A.S. Botvina, and D.H.E. Gross, Nucl. Phys. A 592 (1995) 257-270.

[7] A.S. Botvina, M. Bruno, M. D'Agostino, and D.H.E. Gross. Phys. Rev. C 59 (1999) 3444-3447.

[8] A.S. Botvina, and I.N. Mishustin, Phys. Rev. C 63 (2001) 061601(R).

[9] M. Jandel, A.S. Botvina, S.J. Yennello, G.A. Souliotis, D.V. Shetty, E. Bell, and A. Keksis. Journal of Physics G:Nucl. Part. Phys. 31 (2005) 29-37.

[10] G.A. Souliotis, A.S. Botvina, D.V. Shetty, A.L. Keksis, M. Jandel, M. Veselsky, S.J. Yennello. Phys. Rev. C 75 (2007) 011601.

[11] A.Ergun, H. Imal, N. Buyukcizmeci, R. Ogul, A.S. Botvina, Phys. Rev. C **92**, 014610 (2015).

[12] Buyukcizmeci N., A.Ergun, H. Imal, R. Ogul, A.S. Botvina, Nuc. Sci. And Tech. 26, S20507 (2015)

[13] H. Imal, A.Ergun, N. Buyukcizmeci, R.Ogul, A.S. Botvina, W. Trautmann, PRC **91**, 034605 (2015).

THANKS FOR YOUR ATTENTION